

A METHOD FOR THE CALCULATION OF THE DYNAMIC FRACTURE TOUGHNESS BASED ON CRACK TIP KINEMATICS

G. Kotsinis^{1*}, T. Loutas¹, G. Sotiriadis¹

¹Department of Mechanical Engineering and Aeronautics, University of Patras, Rio-Patras, Greece

* Corresponding author (kotsinisgeorgios@gmail.com)

Keywords: Split Hopkinson Pressure Bar, High Speed Loading, Strain Energy Release Rate

ABSTRACT

In this work a study for the selection of the more appropriate beam theory-based kinematic assumptions to describe the through the thickness kinematics of an adhesive joint or laminated beam in all its length will be presented. The scope is the use of the beam theory-based kinematic assumptions for the calculation of the fracture toughness expressed by the J -integral based on data from a Digital Image Correlation analysis. The cases of the path independent J -integral and the path dependent generalised J -integral are studied. Three different kinematic assumptions are considered to describe a Double Cantilever Beam specimen: the Timoshenko beam theory, a Layerwise model and a semi-Layerwise model. The best use of each model is highlighted for nine study cases. Finally, a discussion is presented on how the Digital Image Correlation analysis data points from experiments, that will be inserted into an analytical model, must be chosen to be compatible with the assumptions of the subsequent data reduction scheme. For the comparison with the experimental results, data for the displacements from a high-speed loading mode I via a Split Hopkinson Pressure Bar apparatus will be used. The Wedge Insert Fracture method was used on Double Cantilever Beam specimens of a metal-composite joint.

1 INTRODUCTION

The use of composites on a large scale has increased the need for a thorough understanding of their mechanical behavior, not only under quasi-static but in elevated loading rates, i.e., dynamic loading/impact, as well. To secure the structural integrity of a structure made by laminated materials under various loading conditions, the interlaminar fracture toughness must be found in order to investigate the most common failure mode of laminated materials. The J -integral [1] is commonly used for the calculation of the fracture toughness of beam-type delamination specimens (Fig. 1a) like the composite laminates and the adhesive joints subjected to a variety of loading rates. When the loading rate is significant the generalized J -integral or crack tip energy flux integral is used for the calculation of the fracture toughness [2]. To calculate the J -integral or the generalized J -integral kinematics, such as displacements and rotations, of the specimen must be used based on the selected integration path. That kinematics can be calculated based on analytical models or via experimental methods like the Digital Image Correlation (DIC) method.

In this work we are focus on the combination of the J -integral or the generalized J -integral with the DIC method for the calculation of the fracture toughness of beam-type delamination specimens. The main idea is to create a method that can be used regardless the loading condition the specimen type and the integration path. This need exists due to the fact that in some cases in order to add considerations for extra phenomena, like the high-speed loading conditions [3-4] considering the vibrational response of the specimen the analytical solutions are quite complex especially when non-common fracture specimens are used. But also, it will be a useful tool for the calculation of fracture toughness. The first step for that is to select the beam theory-based kinematic assumptions to model the kinematics of the specimen. The main capability of the selected model is to describe (Fig. 1b) the kinematic field obtained from the DIC in order the input data to be compatible (the values of the measurement points could theoretically be calculated analytically, Fig. 1b) with the analytical assumptions. It must be mentioned that in some cases a model cannot describe the kinematic field but there are compatible points (Fig. 1b).

In a recent work [4], the authors comment on the importance of the correct selection of the data points from DIC.

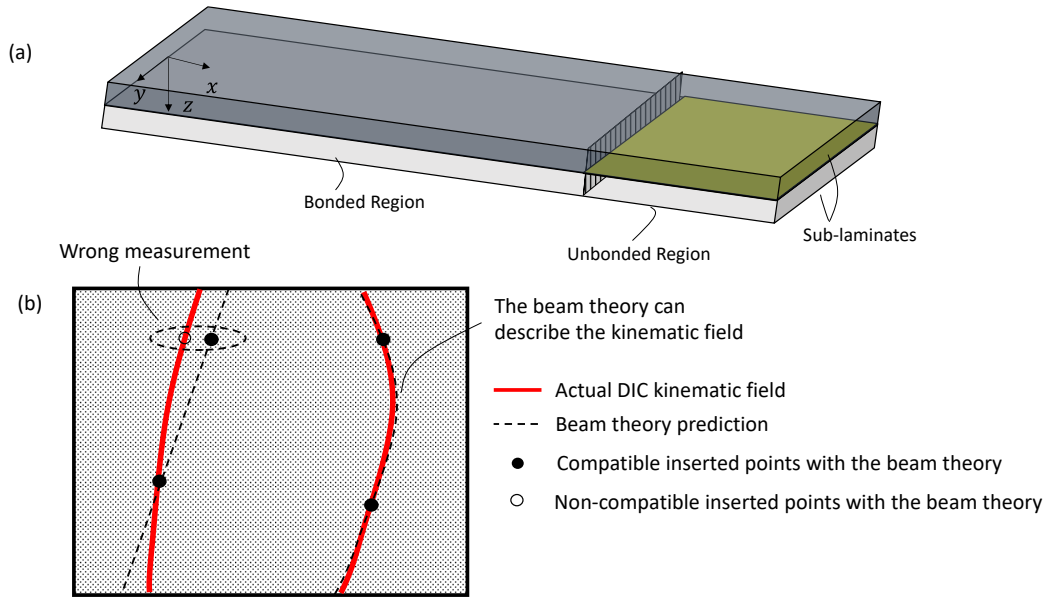


Figure 1: a) Graphical representation of some terms used in the manuscript, b) The compatibility of the points

In the next sections we study three different beam theory-based kinematic assumptions. Each one more complex than the other. The capabilities of each will be presented based on nine case studies for a Double Cantilever Beam (DCB) specimen. Since the calculation of the generalized J -integral is the main outcome, the DIC extracted kinematic field from a DCB specimen loading under high-speed loading will be also used to find the best analytical model. Although the outcome of the paper is also useful for static loading conditions. In the next paragraph we analyse the conditions for which data from a DIC analysis can be imported into a formula from the fracture toughness, calculated based on a contour integral, using beam theory-based kinematic assumptions.

The formula for the fracture toughness, using a contour integral, is calculated as a function of the specimen kinematics and their derivatives, based on the assumptions of an analytical model. Most analytical models in the literature use two main assumptions to model a beam-type delamination specimen: 1. A beam theory, 2. An interface assumption (clamped, rigid, semi rigid, elastic [5]). When we want to use an analytical formula for the fracture toughness but instead of calculating the variables (e.g., kinematics) analytically, we introduce them experimentally, we must make sure that the introduced variables are compatible with the analytical model. In other words, the selected data from the DIC should be the same or similar as what the analytical model would produce. For that two cases occur: 1. The analytical model can capture the full field kinematics of the DIC analysis (especially the through the thickness variation), 2. The inserted DIC points could theoretically be calculated by the analytical model. A simple example for the second point is the transverse deflection on the crack tip coordinate of a similar (same material at each sub-laminate) and symmetric (same thickness at each sub-laminate) DCB specimen. If the analytical model from [4] will be used for example, the analytical value of the deflection on the crack tip coordinate will be zero. Thus, if a formula based on this model was used for the fracture toughness to implement data from the DIC, the results would be misleading because at the midplane of the DIC analysis the deflection is not equal to zero. Although the model in [4] is capable to calculate the fracture toughness on its own. This phenomenon occurs because the analytical models are capable to describe the strain energy of the specimen and thus, the fracture toughness even if they cannot capture the full field kinematics.

To be more clear let's analyse the most common J -integral formula for a DCB specimen [6]:

$$J = \frac{P(w'_u - w'_b)}{b} \quad (1)$$

where: P is the load, b the width of the specimen and w'_u , w'_b are the transverse displacement derivatives for the upper and the lower sub-laminate on the loading points.

Eq.1 provides a simple and elegant solution to calculate the fracture toughness with two assumptions: 1. the specimen can be modelled as an Euler beam (there is no shear effects), 2. the method by which the derivative is calculated experimentally from the DIC. The first assumption refers to the validity of Eq. 1 to model the specimen and the second one on the selection of the material points in order to be compatible with the beam theory used.

ESL beam theories, like Euler's and Timoshenko's, calculate the beam kinematics based on the beam's midplane and assume a linear distribution of the axial displacements and a constant distribution for the transverse displacements. Although the DIC software provides a 2D displacement field in which the displacements vary in an arbitrary way through the beam's thickness. Eq. 1 can be used *if the through the thickness transverse displacement on the loading point during the experiment remains constant* in order, then to calculate the derivative as a finite difference. The calculation of the derivative for the Eq. 1, can use the axial displacements of two vertical points. By that, the definition of w' becomes coincident with the kinematic rotation φ of the Timoshenko theory. Thus, the shear effects are also included. In this case the axial displacement *must be linear through thickness*.

Thus, the following statement will be investigated, *data points from a DIC analysis can be used on a J -integral formula only if the beam theory-based kinematic assumptions can capture accurately the through the thickness distribution of the displacements or at least the measurement points are compatible with the beam theory-based kinematic assumptions.*

2 THEORETICAL BACKGROUND

2.1 The J -integral

In this section the formulas for the J -integral and the generalized J -integral are presented. For the generalized J -integral the cases for which the integral is path independent are also pointed out.

The most common expression for the J -integral referred also as *static* J -integral is given as [6]:

$$J = \int_{\Gamma} \sigma_{kl} \hat{n}_l \frac{du_k}{dx} + U^d \hat{n}_1 \quad (2)$$

The generalized J -integral or crack tip energy flux integral is given as [2]:

$$J = \lim_{\Gamma \rightarrow 0} \frac{\int_{\Gamma} \sigma_{kl} \hat{n}_l \frac{du_k}{dt} + (U^d + T^d) c \hat{n}_1}{c} \quad (3)$$

where: σ_{kl} , u_k , are the stress and displacement tensors, \hat{n} , is the normal unit vector and c , is the velocity of the crack and U^d , T^d , are the strain and kinetic energy density.

In case of mixed mode loading the individual components of the fracture toughness can be calculated by separating the stresses, strains and the displacements into symmetric and antisymmetric fields [7].

The J -integral is a path independent integral [6]. The generalised J -integral in general is not path independent, except in the immediate vicinity of the crack tip [7]. A case that the integral is indeed path-independent is in steady state conditions, such as the propagation of a crack with constant velocity. But in this case the only relation between the problem variables (kinematics, strains, stresses) and the time variable is by the relation $\xi = x - ct$ where ξ is the coordinate travelling with the crack tip and c is the velocity of the crack tip [7]. This assumption can be achieved in a very close region to the crack tip. But if no crack propagation is assumed the initiation fracture toughness can be calculated by a path independent integral *if* the problem variables are independent of time. Recent studies [3-4] show the dependency of the fracture toughness on the vibrational characteristics of the specimens. In this case the problem variables are dependent on the time variable even before crack propagation.

The total derivative $\frac{du_k}{dt}$ from Eq. 3 can be expressed as:

$$\frac{du_k}{dt} = -c \frac{\partial u_k}{\partial x} + \frac{\partial u_k}{\partial t}. \quad (4)$$

Then, three cases arise:

1. when $\frac{\partial u_k}{\partial t} = 0$ the generalized J -integral is equal to the static J -integral [6].
2. when the crack propagates the $\frac{\partial u_k}{\partial x}$ is dominate on the $\frac{\partial u_k}{\partial t}$ term close to the crack tip [6] thus, for crack propagation the J -integral is path independent only near the crack tip area.
3. when no crack propagation is assumed but the specimen has a vibrational response the equality $\frac{du_k}{dt} = -c \frac{\partial u_k}{\partial x}$ is valid only close to the crack tip.

The third point can be proved by using the analytical expressions for the kinematics of a DCB specimen considering the vibrational response from [4]. It must be mentioned that if no crack propagation is assumed to have occurred the c is set equal to zero at the final stage of the calculations not directly on Eq. 4 [4]. Thus, *when the elastic vibration is considered the integration path must be close to the crack tip even for crack initiation.*

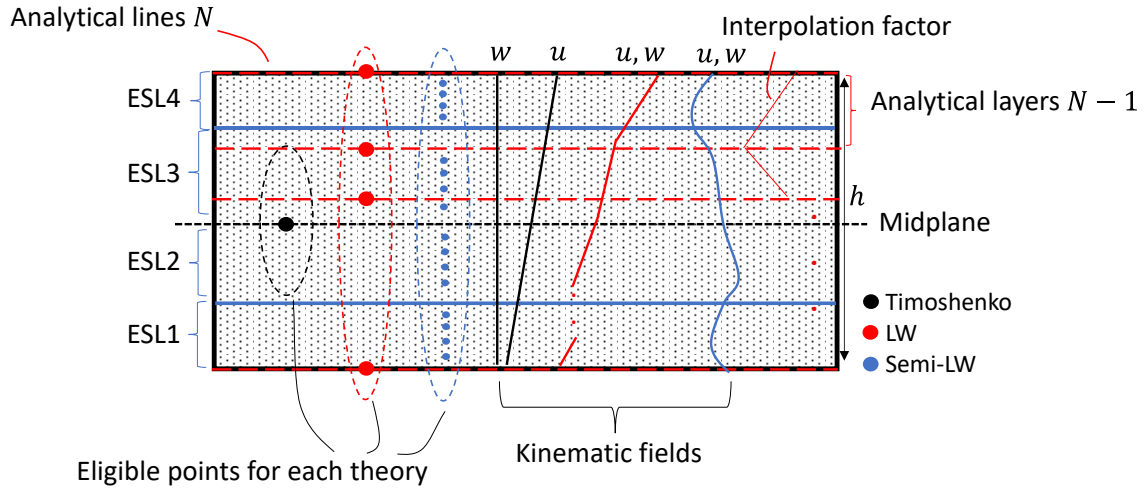


Figure 2: A beam element that contains terminologies, the eligible points and the distribution of the displacements for each beam theory-based kinematic assumptions

2.2 Presentation of the beam theory-based kinematic assumptions

Three beam theory-based kinematic assumptions will be used in this work. The first one is the well-known Timoshenko's beam theory [8] the second one is a Layerwise (LW) theory with linear interpolation factors [9] and the third is a semi-Layerwise theory (semi-LW) [10], as originally proposed by Szekrényes, which consists of several Equivalent Single Layer (ESL) theories jointed together with constraints, each ESL can have different kinematic assumptions.

For the Timoshenko theory the kinematics are expressed as [7]:

$$u(x, z, t) = u_o(x, t) + z\varphi(x, t), \quad (5)$$

$$w(x, z, t) = w_o(x, t). \quad (6)$$

where: u, w are the axial and transverse displacement, u_o, w_o are the membrane displacements and t is the time variable. The kinematic field is presented in Fig. 2.

The inserted points must be calculated on the midplane for the axial and the transverse displacement (Fig. 2). The rotation can be calculated by using two vertical points as $\varphi = (u_1 - u_2)/h$ or by the assumption $w' = \varphi$ [11]. A major problem with the Timoshenko theory is the constant variation of the transverse displacement thus, only one point can be compatible for the transverse displacement and two for the axial.

To solve that problem, a linear variation in the transverse displacement through thickness can be achieved by the following LW model is [9]:

$$u(x, z, t) = \sum_{I=1}^N U^I(x, t)\Phi^I(z), \quad (7)$$

$$w(x, z, t) = \sum_{I=1}^N W^I(x, t)\Phi^I(z). \quad (8)$$

where: U^I, W^I are the axial and transverse displacement of the I analytical layer, N is the total number of the analytical layers (in LW theories the terms nodes and numerical layers are commonly used due to their implementation on finite elements. But in this work due to the analytical approach, we use the term analytical lines and layers to avoid confusion) and Φ is the linear interpolation factor (Fig. 2). The inserted points must be calculated at each analytical line (Fig. 2). This model gives the advantage that 2 points can be at the same time compatible in both displacements even with the use of one layer. Using more layers, the full field can be captured but also more DIC points must be used.

The formula for the J -integral can then be expressed as:

$$J = \sum_{I=1}^N -\widetilde{Q}_x^I \frac{\partial W^I}{\partial x} - N_{xx}^I \frac{\partial U^I}{\partial x}. \quad (9)$$

where: $\widetilde{Q}_x^I, N_{xx}^I$ are the stress resultants in each analytical line which can be expressed based on the applied load. Thus, Eq. 6 can be calculated only by the load and the kinematics.

One major drawback is that if more layers are used the calculation of the J -integral becomes quite rigorous. If higher order interpolation factors are used the number of the analytical lines will be too large. Also points at the boundaries of the specimens are needed which are difficult to be calculated by the DIC [12].

To achieve variations in displacements up to a 3rd order polynomial without the use of many layers the following kinematic field is assumed [10]:

$$u_i(x, z_i, t) = u_0(x, t) + u_{0_i}(x, t) + \theta_{x_i}(x, t)z_i + \phi_{x_i}(x, t)z_i^2 + \lambda_{x_i}(x, t)z_i^3, \quad (10)$$

$$w_i(x, z_i, t) = w_0(x, t) + w_{0_i}(x, t) + \theta_{z_i}(x, t)z_i + \phi_{z_i}(x, t)z_i^2 + \lambda_{z_i}(x, t)z_i^3. \quad (11)$$

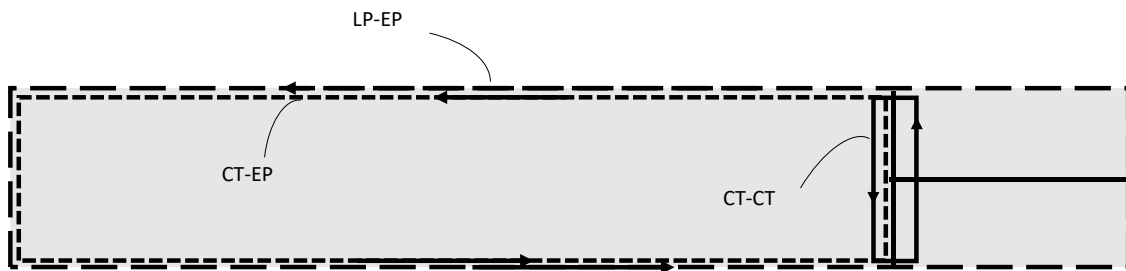
where: u_0, w_0 and u_{0_i}, w_{0_i} are the global and local membrane displacements respectively, $\theta_{x_i}(x), \theta_{z_i}(x)$ are rotations based on the x and z axes and $\phi_{x_i}, \phi_{z_i}, \lambda_{x_i}, \lambda_{z_i}$ are higher order rotations. In this form (Eq. 10-11) the kinematic field is described by a third-order shear deformation theory (TSDT) with cubic stretching but it can also be described with more simple models by eliminating the higher order terms. In this work two ESL theories will be used in each sub-laminate. For the semi-Layerwise model the number of points used is related with the order of the ESL that will be used. For Eq. 10,11 at least four points must be measured for each ELS, thus sixteen points in total. If the variations between those points can be described by the polynomial order of kinematics (Eq. 10-11), then those points are compatible with the analytical model and the through the thickness kinematics can be described by the analytical model. Those points can be fitted thus, the problem with the boundary points is not necessary. The J -integral formula will be discussed in a latter publication by the authors.

2.3 Capabilities of each beam theory-based kinematic assumptions

In this section the capabilities of each model will be investigated, using the following nine cases (Fig. 3 a, b) for a DCB specimen:

1. Similar symmetric LP (Loading Point) -EP (End Point) Path
2. Similar symmetric CT (Crack Tip)-EP Path
3. Similar symmetric CT-CT Path
4. Similar symmetric ($B \neq 0$) LP-EP Path
5. Similar symmetric ($B \neq 0$) CT-EP Path
6. Similar symmetric ($B \neq 0$) CT-CT Path
7. Dissimilar asymmetric LP-EP Path
8. Dissimilar asymmetric CT-EP Path
9. Dissimilar asymmetric CT-CT Path

Where B is the axial-bending coupling matrix. The CT-CT Path is referred to the generalized J -integral. The first six cases are pure mode I loading and the last three mixed mode loading. In **Figure 3** the kinematic distributions are presented, as they result from a simple FE analysis which is not included in this work for brevity.



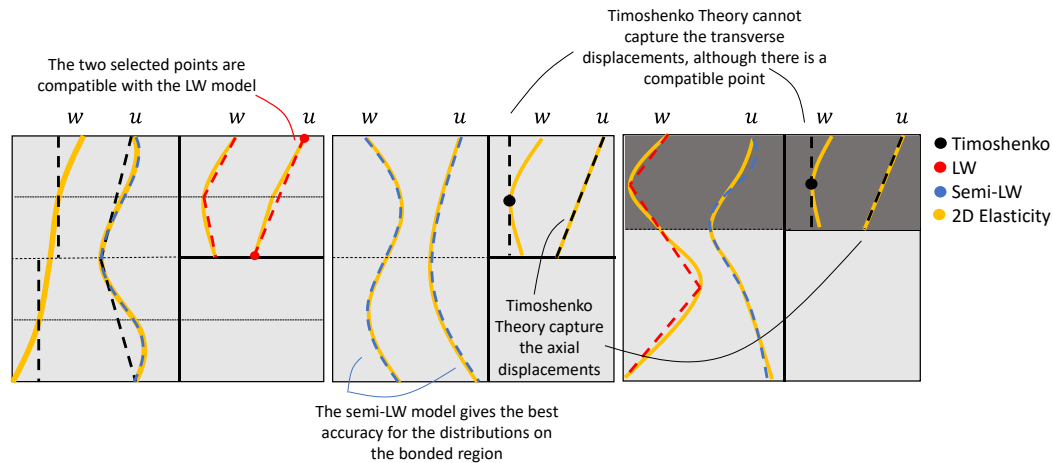


Figure 3: a) Presentation of the different integration paths, b) Kinematic fields comparison

Regarding the LP-EP path Timoshenko theory can be used because at the loading point the kinematics distribution can be captured accurately. Away for the crack tip even for the *cases 4,7* the distribution of the axial displacements its linear and the transverse displacement has a quite constant value because the effect of the higher-shear orders is small. The results for that cases are not presented for brevity. The Timoshenko theory is also able to be used for *case 2,8* if the following is made: $\varphi \cong w'$ because only the rotations can be captured correctly (Fig. 3). In all these cases the other two theories can also be used but Timoshenko theory gives simpler solutions. The only case that the Timoshenko model cannot be used in these cases is for specimens with very large thicknesses like composite sandwich specimens.

The LW approach is very handy to calculate the total fracture toughness using elegant solutions in cases like *case 5* even with only one analytical layer in every adherent.

For the rest of the cases (*case 3,6,9*) the semi-LW theory can be used. Even if Timoshenko theory can capture the total fracture toughness in *case 7,8* to calculate the individual components a path close to crack tip must be used in order to have more accurate results [7]. Thus, *the semi-LW approach dominates when mixed mode fracture is studied and when expressions based on the generalized J-integral are used.*

Table 1 gives in brief the best use of each theory.

	Advantages	Disadvantages
Timoshenko	<ul style="list-style-type: none"> Elegant solutions for cases 1, 4 	<ul style="list-style-type: none"> Cannot be used for the generalized <i>J</i>-integral Cannot be used for mode partitioning Cannot be used if the kinematics distributions are not following the theories assumptions
LW	<ul style="list-style-type: none"> Elegant solutions for cases 1,2, 4, 5 (without to be a function of the elastic properties) 	<ul style="list-style-type: none"> Lots of layers are needed to capture more complex kinematic fields

		<ul style="list-style-type: none"> • Points at the boundaries of the specimen are needed which are difficult to be calculated.
Semi-LW	<ul style="list-style-type: none"> • Usable in all nine cases • Can provide direct mode partitioning • It's the only model that can be used for generalized J-integral 	<ul style="list-style-type: none"> • Needs a lot of DIC points and good measuring accuracy

Table 1: Advantages and disadvantages of each model

3 THE EXPERIMENTAL SET-UP

The above theoretical framework was applied to a case of a metal-composite adhesive joint. The metal-composite adhesive joint under-investigation consists of two adherents: one consisting of a titanium sheet and the other a woven composite. Two aluminum backing beams were added to prevent the plastic deformation of the titanium sheet during testing. The testing in mode I loading was executed in a Split Hopkinson Pressure Bar (SHPB) apparatus. For the mode I test the Wedge Insert Fracture method (WIF) was used on Double Cantilever Beam (DCB) specimens (Fig. 4). The displacement rate and the crack initiation time was measured using a high-speed camera. To avoid any artificial vibration of the specimen the camera was mounted on the configuration. For the DIC pattern a controlled airbrush was used to create the desirable speckle size after a trial-and-error procedure. During the experiments a constant loading velocity was achieved on each sub-laminate.

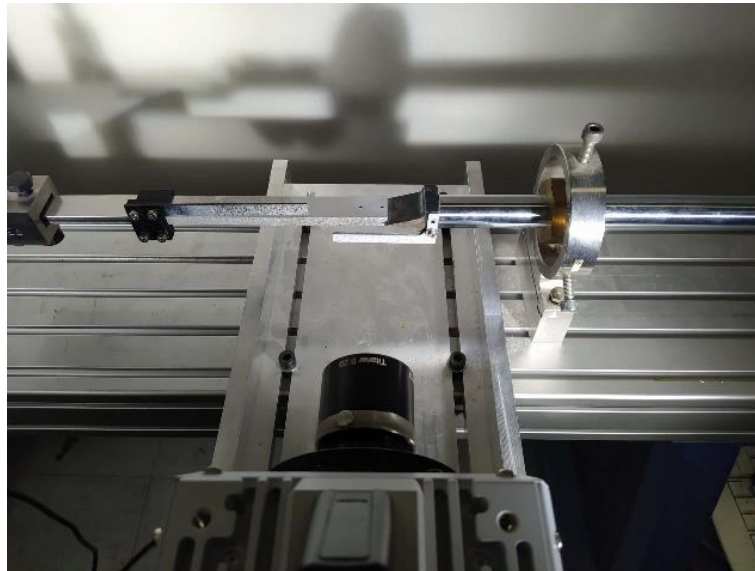


Figure 4: The experimental set-up

4 COMPARISON WITH EXPERIMENTAL RESULTS

The kinematic field as obtained from the DIC analysis for the axial and the transverse displacements is presented on Fig. 5a:

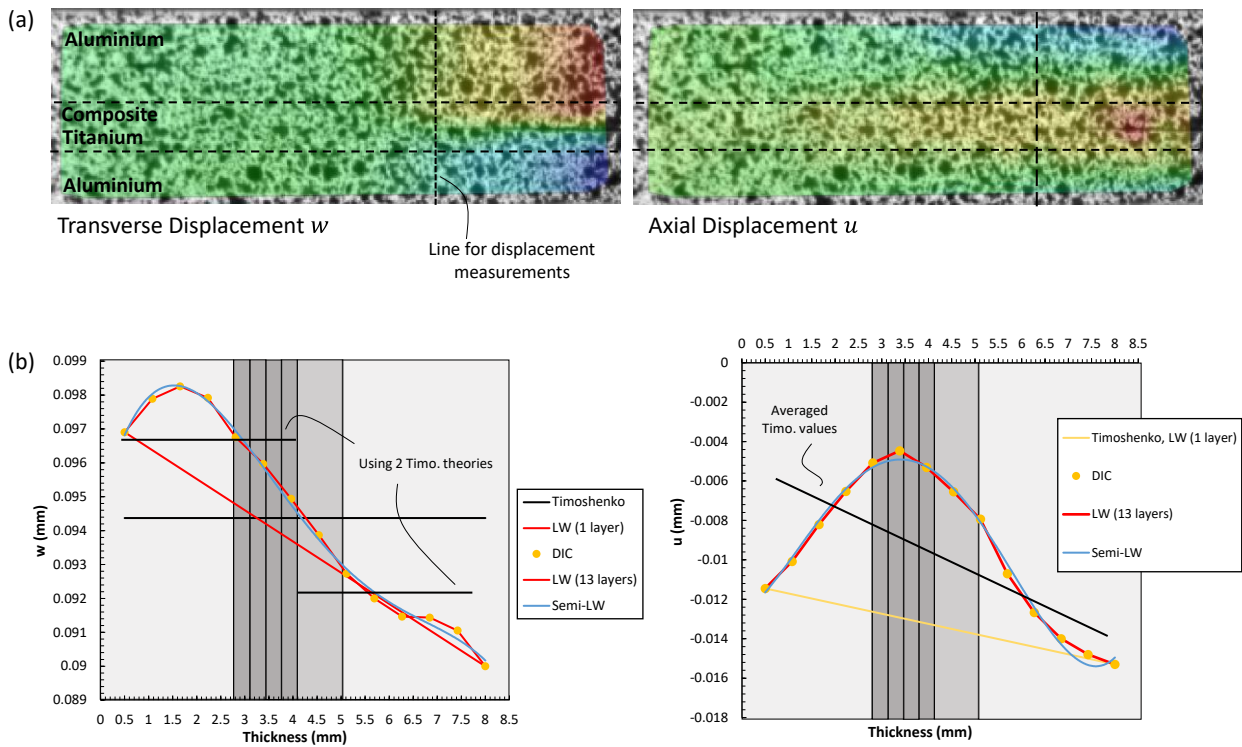


Figure 5: a) The DIC obtained kinematic field b) Use of each model to describe the DIC results

The DIC analysis was performed on the commercial software GOM Aramis with a facet size equal to 15 pixels to follow the rule of 3-7 pixels into a speckle [3]. A Photron® Fastcam SA4 at 60000 fps was used with a resolution of 320x160 pixels. The shutter speed was set according to the frames per second. 1 μ m accuracy was achieved, calculated using a static video [12]. Points close to the boundaries are excluded due to the facet size [12]. It must be mentioned that a small rigid body motion was observed in the results for the axial displacements but it does not affect the results. Also, the transverse displacement is not symmetric by the crack tip due to the dissimilarity and the asymmetry of the adhesive joint.

Then each model was used to investigate if it can describe the DIC obtained kinematics. As presented on Fig. 5b the Timoshenko beam model cannot capture both axial and transverse displacements. The LW model can be used for the calculation for the total fracture toughness since two points are compatible with the DIC kinematics but to capture the individual mode contributions, in which the full field is needed, 13 layers must be used. The semi-LW can be fitted with great accuracy with the results, using Eq. 10-11. Since using Eq. 9 for 13 layers is more rigidus. The semi-LW model will be the one with which the fracture toughness will be calculated in the later stages of this work.

5 CONCLUSIONS

In this work three beam theory-based kinematic assumptions were studied in order to be used for the experimental calculation of the fracture toughness using DIC kinematics. The main conclusion of this work is:

- Data points from a DIC analysis can be used in a J -integral formula only if the beam theory-based kinematic assumptions can accurately capture the through the thickness distribution of the displacements or at least if the measurement points are compatible with beam theory-based kinematic assumptions.

The conclusions regarding the analytical models are:

- The semi-LW model has the best capabilities and spectrum of applicability and is proposed as the solution for the calculation of the generalized J -integral in high-loading speed delamination scenarios and also for the cases when mixed mode loading conditions exist. An added advantage is the ability to calculate the individual components for the fracture toughness
- The best use for the LW model is the problem of *case 5*.
- When the Timoshenko beam model is used the user must be very careful in order to not surpass the limitations and the assumptions of the model

ACKNOWLEDGEMENTS

This article is based upon work from COST Action CA18120, supported by COST (European Cooperation in Science and Technology).

REFERENCES

- [1] J.R. Rice, A Path Independent Integral and the Approximate Analysis of Strain Concentration by Notches and Cracks. *Journal of Applied Mechanics*, **35**, 1968, pp. 379–386
- [2] L.B. Freund, *Dynamic Fracture Mechanics*, Cambridge University Press, 1990
- [3] T. Chen, C.M. Harvey, S. Wang, V.V. Silberschmidt, Dynamic interfacial fracture of a thin-layered structure, *Procedia Struct. Integr.*, **13**, 613–618, 2018. (<https://doi.org/10.1016/j.prostr.2018.12.101>).
- [4] G. Kotsinis, T. Loutas, Strain energy release rate under dynamic loading considering shear and crack tip root rotation effects. *European Journal of Mechanics, A/Solids*. 2022 Mar 1;92 (<https://doi.org/10.1016/j.euromechsol.2021.104435>).
- [5] Qiao, P., Wang, J., Novel joint deformation models and their application to delamination fracture analysis. *Compos Sci Technol*, **65**, 1826–1839, 2005. (<https://doi.org/10.1016/j.compscitech.2005.03.014>)
- [6] T. L. Anderson, *Fracture Mechanics: Fundamentals and Applications, Fourth Edition*, CRC Press, 2017
- [7] M. Kuna, *Finite Elements in Fracture Mechanics*, vol. 10. Springer, Berlin, 2013
- [8] S. Timoshenko, *Theory of Elasticity by Timoshenko*, second ed. McGraw-Hill, New York. 1951.
- [9] J.N. Reddy, *Mechanics of Laminated Composite Plates and Shells: Theory and Analysis*, second ed. CRC Press, Boca Raton, 2004.
- [10] A. Szekrényes, Semi-layerwise analysis of laminated plates with nonsingular delamination the theorem of autocontinuity. *Appl. Math. Model.*, **40(2)**, 1344–1371, 2016
- [11] G. Kotsinis, T. Loutas and G. Sotiriadis, Influence of high-rate testing on the interlaminar fracture behaviour of metal-composite joints, Proceedings of the 20th European Conference on Composite Materials (ECCM20), Lausanne, Switzerland, June 26-30, 2022, EPFL Lausanne, Composite Construction Laboratory, 2022 (https://doi.org/10.5075/epfl-298799_978-2-9701614-0-0).
- [12] International Digital Image Correlation Society, E.M.C Jones, M.A. Iadicola., *A Good Practices Guide for Digital Image Correlation*, 2018 (<https://doi.org/10.32720/idics/gpg.ed1>). (<https://doi.org/10.1016/j.jmps.2018.08.013>)